Chemical-state studies of Zr and Nb surfaces exposed to hydrogen ions

T. A. Sasaki and Y. Baba
Department of Chemistry, Japan Atomic Energy Research Institute, Tokai-mura, Ibaraki-ken 319-11, Japan
(Received 6 December 1983; revised manuscript received 23 July 1984)

Surface chemical states were studied for Zr and Nb metals exposed to 8-keV hydrogen molecular ions. X-ray photoemission spectroscopy (XPS) measurements revealed that chemical shifts of the binding energies for the ion-implanted Zr from the metallic states are 0.6—1.4 eV, consistent with the core-line shifts for thermally synthesized $ZrH_{1.64}$. In the case of the ion-implanted Nb, the corresponding shifts are 0.6—0.8 eV, in good agreement with those for thermally synthesized $NbH_{0.86}$. On the other hand, the ion implantation provided XPS spectra with a distinct photopeak attributable to a metal $4d$—H $1s$ bond near the Fermi level, 3.4 eV for Zr and 4.6 eV for Nb, respectively. The peak positions are $\sim$2.5 eV lower than those calculated previously for the dihydrides. The photopeaks grew upon thermal annealing to 610 °C. The observations are discussed in relation with the peculiarity of hydrogen sites in the crystal lattice and partial recovery of the ion-induced surface damage.

I. INTRODUCTION

Transition metals are capable of absorbing relatively large amounts of hydrogen. Considerable changes in the mechanical (ductile→brittle), thermochemical, and physical properties accompany the hydrogenation of the host metal. In an attempt to understand changes in the electronic structure following hydrogenation, metallic hydrides have been intensively studied from both theoretical and experimental points of view.

Recent theoretical works concerning the electronic structure of metal hydrides[1–7] have shown an appearance of a new intense band several eV below the Fermi level in the calculated density of states. This is attributed to a hydrogen-induced band accompanying the charge transfer from metal to hydrogen.

The first experimental evidence for the existence of hydrogen-induced bonding states has been provided by ultraviolet photoemission spectroscopy for the Pd-H system[8] and for titanium films containing absorbed hydrogen.[9] However, keeping the hydride surface chemically pure is extremely difficult because of both its rapid oxygen adsorption and carbon-containing contaminants.[10–12] Sputter cleaning by the use of an Ar^+ ion may cause changes in the stoichiometry of the hydride, even though the oxide overlayer may be efficiently removed. Filing or scraping in an ultrahigh vacuum involves technical difficulties because the hydrides are fragile. Thus far, x-ray photoemission spectroscopy (XPS) works which are considered to be reliable have been made only for the Zr-H,[11] Ce-H,[13,14] and La-H (Ref. 15) systems.

This paper describes XPS studies of the metal-hydrogen bond in zirconium and niobium hydrides which are formed on the metal surfaces by implantation of energetic hydrogen ions. Thermally synthesized $ZrH_{1.64}$ and $NbH_{0.86}$ which decompose at high temperatures are used for confirmation of the core-line energies of the hydrides. In addition, valence-band (VB) spectra obtained are compared with recent calculations.[5] Anomalies of the VB spectra found in thermal annealing experiments are discussed in connection with recovery of the lattice distortions in ion-induced damage layers.

II. EXPERIMENT

A. Materials

Starting materials were 99.9% metallic foils from Furuuchi Chemical Co., Ltd. The thermal synthesis of the hydrides was essentially the same as those described by Veal *et al.*[11] and Wainwright *et al.*[16] Briefly, metallic foils in a molybdenum boat were degassed at 650 °C for 15 h in an electric furnace at a pressure $\leq 2\times10^{-6}$ Torr. Keeping the furnace at 570 °C, purified H_2 gas was introduced to a pressure of 1.2 atm. Then the furnace was cooled over a period of 30 min to 350 °C and evacuated to a pressure of $\sim10^{-6}$ Torr. Subsequently, the furnace was again heated to 570 °C. By repeating this procedure three times the metallic foils were extremely activated for the hydrogenation.

The chemical compositions of the hydrides obtained were determined to be $ZrH_{1.64}$ and $NbH_{0.86}$ by gravimetric methods. Before introduction into the spectrometer chamber, the hydrides were carefully polished with emery paper in a dry-nitrogen atmosphere to decrease surface contaminants.

Reference materials of the metallic oxides were prepared by oxidizing zirconium hydroxide and Nb foil at 1000 °C. Niobium dioxide, which was also used as a reference material, was obtained by reducing Nb_2O_5 with hydrogen at 1000 °C.

B. Ion-implantation method

Before the implantation, the metallic foils were annealed at 550 °C at a pressure $\leq 5\times10^{-9}$ Torr. They were then mechanically filed in a preparation chamber at a pressure of 2×10^{-10} Torr.

The ion implantation was done using a Penning-ion-gauge ion gun into which purified H_2 gas continuously flowed. The metallic foils were exposed to 8-keV hydrogen molecular ions (mostly H_2^+) at a pressure of 8×10^{-6} Torr. The current density monitored by the use of a small Faraday cup was 80—150 $\mu A/cm^2$, and the total fluence was $\lesssim 1\times10^{18}$ ions/cm^2.

C. Thermal annealing and XPS measurements

To examine changes in the XPS spectra accompanied by hydrogen evolution, the sample was annealed in the spectrometer chamber to 610 °C and the electric furnace at 1100 °C for 30 min. The pressure was $\sim10^{-6}$ Torr when the thermally synthesized $NbH_{0.86}$ was annealed at temperatures of 420—490 °C, where H_2 gas was released due to the thermal decomposition. On the other hand, the pressure remained below 8×10^{-9} Torr even if the ion-implanted samples were annealed to 610 °C.

XPS measurements were carried out with an ESCALAB-5 spectrometer (V. G. Scientific Co., Ltd.) employing Mg $K\alpha$ x rays (1253.6 eV). The base pressure of the analyzer chamber was less than 2×10^{-10} Torr.

Energies were calibrated using the $4f_{7/2}$ line of metallic gold, assumed to have a binding energy of 84.0 eV. The reproducibility of the measured energies was within ±0.1 eV. Deconvolution of the core-line spectra was essential in the chemical-state analyses of the hydrides thermally synthesized. This was done by means of a Gaussian curve-fitting program.

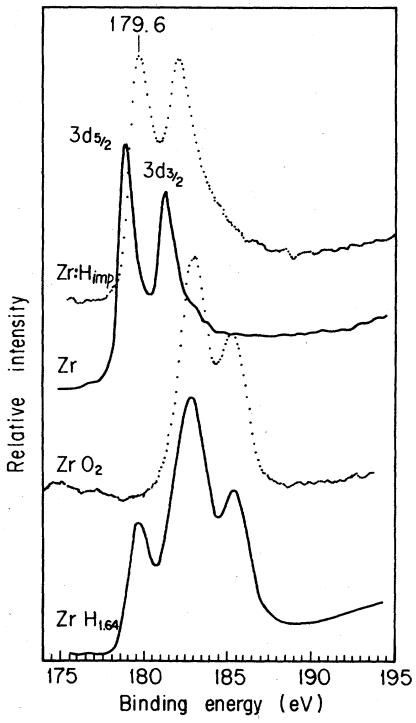

FIG. 1. Zr 3d XPS spectra of Zr:H_{imp}, Zr, ZrO_2, and $ZrH_{1.64}$. Note that the surface of the $ZrH_{1.64}$ sample is covered with a large amount of oxide(s).

III. RESULTS AND DISCUSSION

A. Core-line energies of zirconium hydride

Figure 1 shows the Zr 3d region of the hydrogen-ion-implanted zirconium Zr:H_{imp}. The spectral pattern and peak position of Zr:H_{imp} were independent of the total fluence from 3×10^{17} to 1×10^{18} ions/cm^2. For comparison, the spectra for Zr metal, ZrO_2, and the $ZrH_{1.64}$ sample are also presented. The energy separation of the Zr $3d_{5/2}$ line between Zr metal and ZrO_2 is 4.3 eV, in agreement with the chemical shift previously reported.[11,17] On the other hand, the surface of the $ZrH_{1.64}$ sample was found to be contaminated with a considerable amount of ZrO_2. This was also confirmed from the presence of the intense O 1s line at 531.0 eV. Nevertheless, a distinct 179.6-eV peak of this sample and also of Zr:H_{imp}, in Fig. 1 could be assigned to that from the hydride, because its chemical shift from the metallic state is 0.6 eV, in agreement with a reported value for $ZrH_{1.65}$.[11] Other firm evidence for the presence of the hydride was obtained by heating the $ZrH_{1.64}$ sample at a temperature over thermal decomposition in the vacuum. This treatment brought about the disappearance of the 179.6-eV peak and the appearance of a new photopeak at 179.0 eV attributable to the Zr $3d_{5/2}$ line of the metallic state.

Discrepancy in the signal intensity of the Zr 3d region for Zr:H_{imp} from the spin-orbit coupling ratio is due to the superposed contribution of the oxide overlayer. Monitoring of the O 1s line revealed that the amount of the oxide impurity estimated from the O 1s—to—Zr 3d ratio is about 25% in terms of ZrO_2, though definite structure attributable to the oxide(s) is invisible in the Zr 3d spectrum of Zr:H_{imp}. The formation of the oxide overlayer is presumably due to implantation of O_2^+ ions which may be contained as an impurity in the hydrogen-ion beam.

It is apparent that the XPS in the present work is far more sensitive to the oxide(s) than to the hydride, taking penetration depth of the ions into account. The projected range of an 8-keV O_2^+ ion (4 keV/O atom) is estimated to be less than 50 Å in zirconium metal,[18] while that of an 8-keV H_2^+ ion (4 keV/H atom) is about 200 Å.[19] Thus oxygen ions would be accumulated in the surface layer including the escape depth of the Zr 3d photoelectron, viz., 15 Å. To confirm this assumption, the Zr:H_{imp} surface was etched with a faint beam of a 5-keV Ar^+ ion for 2 min. This treatment made the right-hand side of the Zr $3d_{3/2}$ region for Zr:H_{imp} in Fig. 1 lower and increased the sharpness of the 179.6-eV peak. In addition, an abrupt decrease in the peak intensity of the O 1s line was observed.

The core-line energies of the hydride determined from the Zr:H_{imp} sample and their shifts from the metallic state are summarized in Table I. The chemical shifts of the Zr 4s and Zr 4p lines are fairly large compared with the other core lines. The observation agrees well with the results by Veal *et al.*[11] who have reported 0.7 and 1.0 eV for the chemical shifts of the Zr $3d_{5/2}$ and Zr 4p lines for Zr:$H_{1.65}$, respectively. It is noteworthy that the core-line energies of the present Zr:H_{imp} sample are almost the

TABLE I. Photopeak positions and chemical shifts for hydrogen-ion-implanted zirconium Zr:H_{imp} and niobium Nb:H_{imp}. M = Zr (for columns on the left) or Nb (for those on the right).

Lines	Position (eV) Zr	Zr:H_{imp}	Chemical shift (eV)	Position (eV) Nb	Nb:H_{imp}	Chemical shift (eV)
M 3s	430.2	431.6	1.4	467.1	467.7	0.6
M 3$p_{3/2}$	329.9	330.7	0.8	360.7	361.5	0.8
M 3$d_{3/2}$	181.4	182.0	0.6	205.2	205.9	0.7
M 3$d_{5/2}$	179.0	179.6	0.6	202.4	203.2	0.8
M 4p	27.5	28.9	1.4	31.0	31.7	0.7
M4d–H 1s		3.4			4.6	

same as those of the stoichiometric hydrides, while bombardments of the heavy rare-gas ions sometimes cause a core-line shift to (0.1–0.3)-eV higher binding energy in such metals as Ti (Ref. 20) and Pd.[21]

B. Core-line energies of niobium hydride

Figure 2 shows the Nb 3d region of hydrogen-ion-implanted niobium Nb:H_{imp}, Nb metal, Nb_2O_5, and the $NbH_{0.86}$ sample. The spectral pattern and peak position of NbH_{imp} were independent of the total fluence of the hydrogen ions as in the case of Zr:H_{imp}.

Because of charging effects during the XPS measurement, the spectrum of insulating Nb_2O_5 was found to shift to higher binding energy. Therefore the energy scale was aligned to make the peak position of the Nb $3d_{3/2}$ lines for Nb_2O_5 and for the most oxidized species on the $NbH_{0.86}$ surface coincide. With this alignment, the separation energy of the Nb $3d_{5/2}$ line between Nb metal and Nb_2O_5 is 5.5 eV, in agreement with the chemical shift measured by previous works.[22]

A tailing to the higher binding-energy side and an increase in the full width at half maxima of the Nb 3d spectrum for Nb:H_{imp}, compared with Nb metal, imply that the Nb:H_{imp} surface is composed of several different chemical species. The deconvolution shown in Fig. 3 gives evidence for the presence of NbO_2 and an identified species. Since the photoelectrons from the latter species have the same binding energy as that of a 203.2-eV peak for the $NbH_{0.86}$ sample, the unidentified species is probably the hydride.

To make the identity of the chemical state clearer, the effect of isochronal annealing on surface chemical composition was investigated. The spectral patterns of the core lines for Nb:H_{imp} were independent of annealing temperatures up to 610 °C. On the other hand, the Nb 3d region of the $NbH_{0.86}$ sample yields spectral changes as shown in Fig. 4. The 203.2-eV peak in question shifts by 0.4 eV at 420 °C, where bulk niobium hybride evolves hydrogen gas. Furthermore, decreases in the oxide overlayer and spectral shifts to the lower binding-energy side are observed on raising the annealing temperature. This is due to thermal diffusion of hydrogen to the surface layer, resulting in the reduction of Nb_2O_5 on the $NbH_{0.86}$-sample surface. With annealing at 1100 °C, the most prominent peak appears at

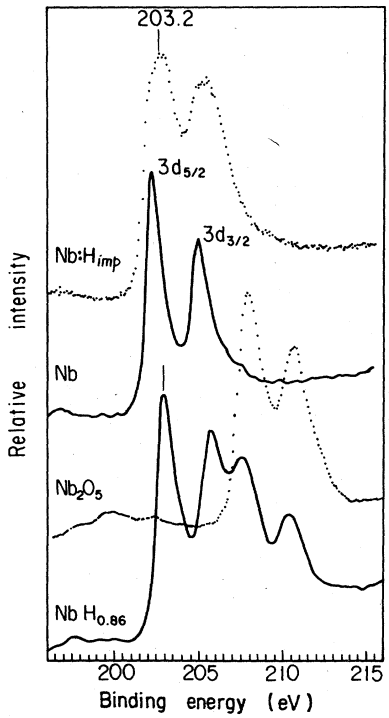

FIG. 2. Nb 3d XPS spectra of Nb:H_{imp}, Nb, Nb_2O_5, and $NbH_{0.86}$. Note that the surface of the $NbH_{0.86}$ sample is covered with a large amount of oxide(s).

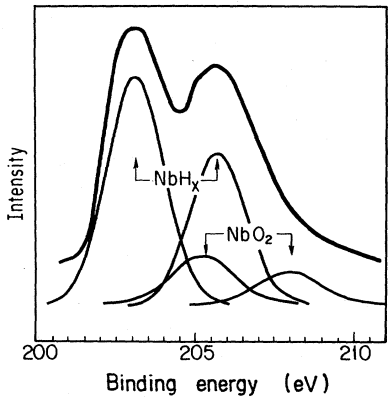

FIG. 3. Deconvolution profile of the Nb 3d region for Nb:H_{imp}.

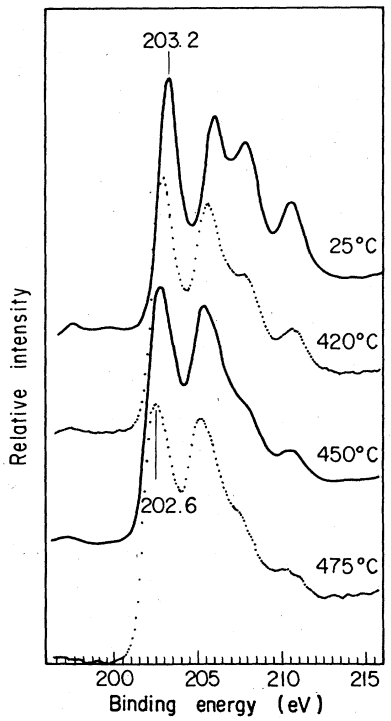

FIG. 4. Spectral changes in the Nb $3d$ region of the $NbH_{0.86}$ sample following isochronal annealing at various temperatures for 30 min.

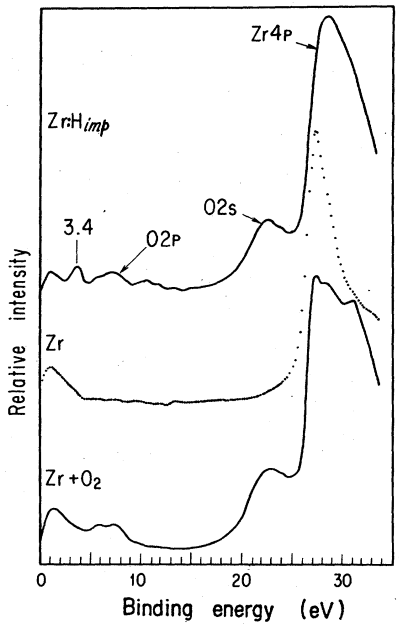

FIG. 5. VB XPS spectra of $Zr:H_{imp}$, Zr, and oxygen-adsorbed Zr. The last sample has been exposed to oxygen until its O $1s$—to—Zr $3d$ ratio becomes equivalent to that of $Zr:H_{imp}$.

202.6 eV, as in the case of annealing at 475 °C. Although the position of the new photopeak disagrees with that of Nb metal, we suppose this is from the metallic phase which has vacancies from the detrapped hydrogen atoms.

The chemical process, $Nb_2O_5 \xrightarrow{\Delta} NbH_x \xrightarrow{\Delta} Nb$, was also reinforced by analyzing changes in the O $1s$—to—Nb $3d$ ratio. Thus the 203.2-eV peaks of the $NbH_{0.86}$ sample and also of $Nb:H_{imp}$ are attributed to the Nb $3d_{5/2}$ line of the hydride.

The core-line energies of the hydride determined from the $Nb:H_{imp}$ sample are listed in Table I. Although the chemical shifts from the metallic states are less than 1 eV, they are larger than the experimental error.

C. Valence-band spectra

Veal *et al.*[11] have found, by means of the data-separation technique, that the Zr—H bond ranges from 4 to 9 eV below the Fermi level. However, our attempt to extract a pure hydride spectrum showed that the reproducibility in the $Zr:H_{imp}$-ZrO_2 separation procedure is not too good because of composite patterns present in the spectra (Fig. 1) from 3 to 9 eV. Therefore, we focus our attention mainly on the new hydrogen-induced photopeak found in the present work.

Figure 5 shows the VB regions for $Zr:H_{imp}$, Zr metal, and oxygen-adsorbed Zr. In order to determine the origin of the ~3.4 eV peak of $Zr:H_{imp}$, the last spectrum was obtained by exposing a clear surface of Zr metal to 7×10^{-7}-Torr O_2 until the O $1s$—to—Zr $3d$ ratio became equivalent to that of $Zr:H_{imp}$. The presence of the well-defined Fermi edge and chemical shift of 1.0 eV in the Zr $4p$ line indicate that the adsorbed surface is composed of the metallic state and ZrO_2. It is also apparent that the oxygen adsorption does not induce any new photopeak at

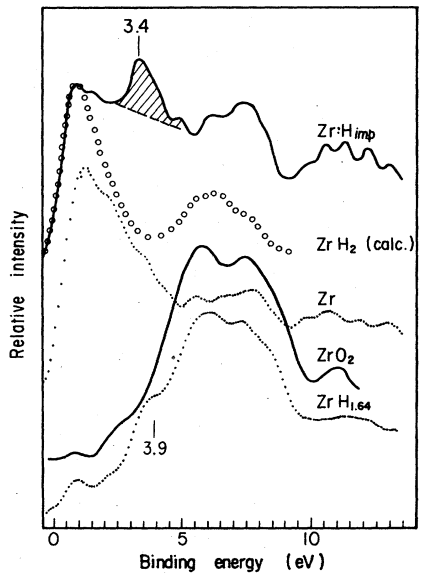

FIG. 6. Blowup of the XPS spectra near the Fermi level of $Zr:H_{imp}$, Zr, ZrO_2, and $ZrH_{1.64}$. The curve using open circles is spectrum calculated for ZrH_2, taken from Ref. 5. The photopeak at 5—9 eV which is observed for all samples is mainly due to oxide(s). The small bump at ~3.9 eV for the $ZrH_{1.64}$ sample is probably from the Zr $4d$—H $1s$ bond.

around 3—4 eV in the binding energy. Furthermore, exposure of Zr metal to 5000-L (1 L=1 langmuir $\equiv 10^{-6}$ Torr sec) H_2 brought about neither core-line shift nor change in the VB region except for the O 2*s* and O 2*p* regions attributable to a small amount of the oxygen contamination. This result is in agreement with the previous observation[23] that both the chemisorption and adsorption at room-temperature result in no hydride formation detectable by the XPS.

An enlargement of the spectrum near the Fermi level of $Zr{:}H_{imp}$ is displayed in Fig. 6 together with those of Zr metal, ZrO_2, and the $ZrH_{1.64}$ sample. The (5—9)-eV photopeak observed for all samples is chiefly due to oxide(s). A small bump at ~ 3.9 eV for the $ZrH_{1.64}$ sample is probably from the Zr—H bond. Open circles represent a spectrum calculated for ZrH_2[5] by means of the discrete-variational $X\alpha$ (DV-$X\alpha$) cluster method. Since damage by (5—10)-keV Ar^+ ion bombardment does not produce any new photopeaks in the VB region of the metal, the photopeak indicated by hatching is attributed to the Zr—H bond. The peak position is in the lower binding energy, compared with the $ZrH_{1.64}$ sample whose main structure of the Zr—H bond would locate at 5—8 eV as previously observed for $ZrH_{1.65}$.[11] The binding energy of ~ 3.4 eV is also smaller by ~ 2.5 eV than the Zr 4*d*—H 1*s* bond calculated for ZrH_2.[5] The appearance of the new photopeak seems to be associated with the difference in the sites occupied by hydrogen atoms. The experimental data obtained for the thermally synthesized hydrides are for the face-centered-tetragonal phase and the calculations for the dihydride with fluorite structure, while the present spectrum is for the hydrogen-ion-implanted surface of Zr metal.

A question may be raised as to why the new photopeak of the Zr—H bond appears in the spectrum of $Zr{:}H_{imp}$. At present, we cannot give a definite answer to this phenomenon. However, one plausible reason is as follows.

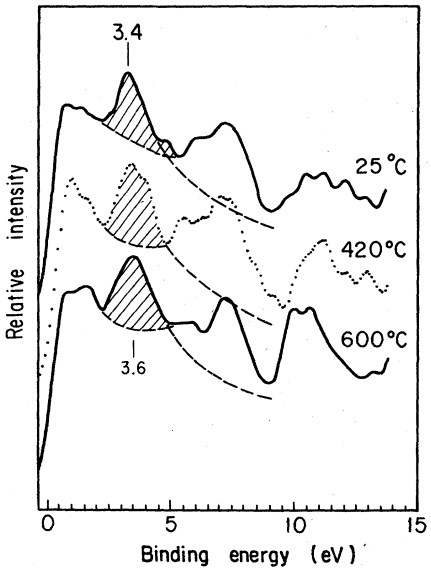

FIG. 7. Spectral changes in the VB region of $Zr{:}H_{imp}$ following isochronal annealing at various temperatures for 30 min.

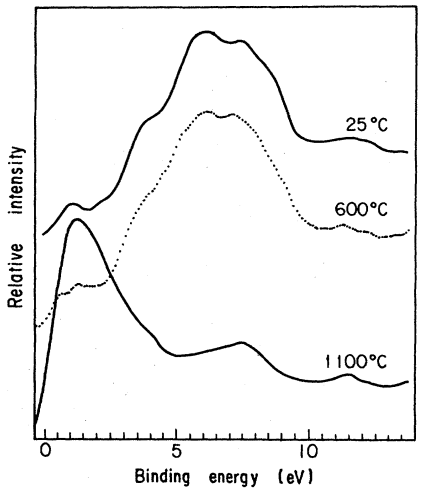

FIG. 8. Spectral changes in the VB region of the $ZrH_{1.64}$ sample following isochronal annealing at various temperatures for 30 min.

The hydrogen atoms may be forced to occupy at the interstitial sites in the hcp lattice of Zr metal. Consequently, the crystal lattice would become distorted. In fact, the DV-$X\alpha$ calculations for a $[Zr_4H_8]$ cluster in ZrH_2 provide molecular-orbital (MO) levels which are sensitive to the bond length between Zr and H atoms. Assuming that the bond length is contracted by 40%, the spectrum has a three-peak structure, 1.6, 3.3, and 5—8.5 eV below the Fermi level. The 3.3-eV peak is split off from the (4.5—8)-eV photopeak with the bonding character of ZrH_2 shown in Fig. 6. Thus, it contains a considerable amount of the H 1*s* character. As a result, the interaction

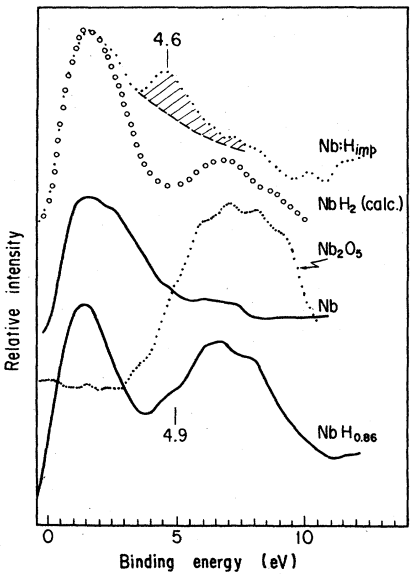

FIG. 9. Enlargement of the XPS spectra near the Fermi level of $Nb{:}H_{imp}$, Nb, Nb_2O_5, and $NbH_{0.86}$. The curve using the open circles is a spectrum calculated for NbH_2, taken from Ref. 5. The small bump at ~ 4.9 eV for the $NbH_{0.86}$ sample is probably from the Nb 4*d*—H 1*s* bond.

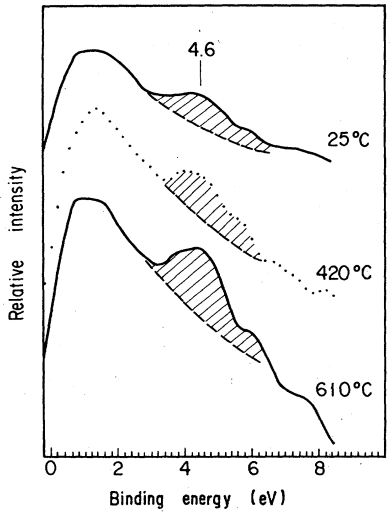

FIG. 10. Spectral changes in the VB region of Nb:H_{imp} following isochronal annealing at various temperatures for 30 min.

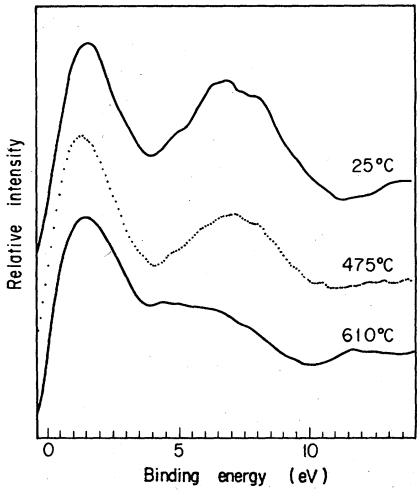

FIG. 11. Spectral changes in the VB region of the $NbH_{0.86}$ sample following isochronal annealing at various temperatures for 30 min.

between the Zr 4*d* and H 1*s* orbitals in the broad peak is diluted, though the strongest interaction still remains at around 5.5 eV. The overall features described above are in reasonable agreement with the spectrum for Zr:H_{imp} in Fig. 6.

As for the distortions, they could be partially removed by thermal annealing. Figures 7 and 8 show the spectral changes in the isochronal annealing for Zr:H_{imp} and the $ZrH_{1.65}$ sample, respectively. One of the most noticeable results obtained is that the peak position of the Zr—H bond in Zr:H_{imp} shifts from 3.4 to 3.6 eV, as seen in Fig. 7. Furthermore, its intensity grows on raising the annealing temperature. These observations are closely related to the partial recovery of the ion-induced distortions of the crystal lattice. On the other hand, the Zr—H bond of the $ZrH_{1.64}$ sample remains almost unchanged until at least 600 °C. The disappearance of the (3—9)-eV spectrum at 1100 °C in Fig. 8 is due to reduction of the oxide overlayer with the hydrogen evolved from the sample itself.

Very similar results were obtained for the Nb-H system. Figure 9 represents the VB spectra of the niobium compounds. The spectral changes in the isochronal annealing of Nb:H_{imp} and the $NbH_{0.86}$ sample are shown in Figs. 10 and 11, respectively. A photopeak at $\sim$4.6 eV indicated by crosshatching in Fig. 9 is attributable to the Nb—H bond. However, the binding energy is lower by at least 0.3 eV than the small bump of the $NbH_{0.86}$ sample and also by $\sim$2 eV than the previous calculations for NbH_2.[3,5,7] In addition, the photopeak of the Nb—H bond becomes sharp with an increase in the annealing temperature, as seen in Fig. 10. On the contrary, the 4.9-eV bump of the Nb—H bond and (5—9)-eV peak of the oxide overlayer of the $NbH_{0.86}$ sample in Fig. 11 decrease on raising the temperature, consistent with annealing behavior of the core-line shift (Fig. 4). Considering that the peak positions of both the core line and Nb—H bond in Nb:H_{imp} remain unchanged, recovery of the crystal structure seems to be incomplete even at 600 °C. If the crystalline distortions are completely removed, the peak positions would shift slightly ($\lesssim$0.3 eV) toward the higher binding-energy side as observed for Zr:H_{imp}.

IV. CONCLUSIONS

Results obtained for hydrogen-ion-implanted Zr and Nb metals may be summarized as follows.

(1) Ion implantation has proved to be quite useful for preparation of hydride overlayers for XPS studies. The chemical shifts of the core lines from the metallic states are 0.6—1.4 eV for zirconium hydride and 0.6—0.8 eV for niobium hydride, in good agreement with those for the thermally synthesized hydrides.

(2) Ion implantation produced a distinct XPS peak near the Fermi level, $\sim$3.4 eV for Zr and $\sim$4.6 eV for Nb, respectively. The hydrogen-induced bands seem to be associated with splitoff from the (5—9)-eV photopeak which is observed in the previous XPS investigation of thermally synthesized $ZrH_{1.65}$ and is also predicted in the previous MO calculations of ZrH_2 and NbH_2.

(3) In thermal annealing to 610 °C, the core-line energies for both Zr:H_{imp} and Nb:H_{imp} remain unchanged, while those for the thermally synthesized $NbH_{0.86}$ shift to the lower binding-energy side attributable to the metallic state. Furthermore, the photopeaks of the metal 4*d*—H 1*s* bond grow on raising the annealing temperature to at least 600 °C. The anomalies observed are probably due to the lattice distortions caused by the ion-induced damage of the surface layers and their partial recovery in the annealing.

[1]A. C. Switendick, Ber. Bunseges. Phys. Chem. **76**, 535 (1972).
[2]M. Gupta and J. P. Burger, Phys. Rev. B **24**, 7099 (1981).
[3]M. Gupta, Phys. Rev. B **25**, 1027 (1982).
[4]A. Fujimori and N. Tsuda, Solid State Commun. **41**, 491 (1982).
[5]T. A. Sasaki and T. Soga, J. Surf. Sci. Soc. Jpn. **3**, 17 (1982).
[6]T. A. Sasaki, J. Surf. Sci. Soc. Jpn. **3**, 182 (1982), and references therein.
[7]D. J. Peterman, D. K. Misemer, J. H. Weaver, and D. T. Peterson, Phys. Rev. B **27**, 799 (1983).
[8]D. E. Eastman, J. K. Cation, and A. C. Switendick, Phys. Rev. Lett. **27**, 35 (1971).
[9]D. E. Eastman, Solid State Commun. **10**, 933 (1972).
[10]V. I. Nefedov, Ya V. Salyń, A. A. Chertkov, and L. N. Padurets, Russ. J. Inorg. Chem. **19**, 785 (1974).
[11]B. W. Veal, D. J. Lam, and D. G. Westlake, Phys. Rev. B **19**, 2856 (1979).
[12]P. S. Wang, R. S. Carlson, and T. M. Wittberg, Mound Laboratory (Ohio, U.S.A.) Report No. MLM-2955, 1982 (unpublished).
[13]L. Schrapbach and J. Osterwalder, Solid State Commun. **42**, 271 (1982).
[14]A. Fujimori and N. Tsuda, Phys. Status Solidi B **114**, K139 (1982).
[15]L. Schlapbach and H. R. Scherrer, Solid State Commun. **41**, 893 (1982).
[16]C. Wainwright, A. J. Cook, and B. E. Hopkins, J. Less Common Met. **6**, 362 (1964).
[17]Y. N. Makurin, V. N. Streskalovskii, and É. G. Vorkorub, J. Struct. Chem. (USSR) **21**, 147 (1980).
[18]K. B. Winterbon, *Ion Implantation Range and Energy Deposition Distributions* (Plenum, New York, 1977), Vol. 2.
[19]H. H. Andersen and J. F. Ziegler, *Hydrogen Stopping Powers and Ranges in All Elements,* edited by J. F. Ziegler (Pergamon, New York, 1977).
[20]Y. Baba and T. A. Sasaki, Japan Atomic Energy Research Institute (Ibaraki, Japan) Report No. JAERI-M-84-005, 1984 (unpublished).
[21]S. Hufner, G. K. Wertheim, and D. N. E. Buchanan, Chem. Phys. Lett. **24**, 527 (1974).
[22]R. Fontaine, R. Caillat, L. Feve, and M. J. Guittet, J. Electron Spectrosc. Relat. Phenom. **10**, 349 (1977).
[23]R. L. Tapping, J. Nucl. Mater. **107**, 151 (1982).